EFDA–JET–PR(10)49

S. Saarelma, A. Alfier, Y. Liang, L. Frassinetti,
M. Beurskens, S. Jachmich, H. R. Koslowski, P. Lang,
R. Pasqualotto, Y. Sun, C. Wiegmann, T. Zhang
and JET EFDA contributors

Density Pump-out Compensation during Type-I ELM Control Experiments with n = 1 Perturbation Fields on JET

Density Pump-Out Compensation during Type-I ELM Control Experiments with n = 1 Perturbation Fields on JET

S. Saarelma[1], A. Alfier[2], Y. Liang[3], L. Frassinetti[4], M. Beurskens[1], S. Jachmich[5], H.R. Koslowski[3], P. Lang[6], R. Pasqualotto[2], Y. Sun[3], C. Wiegmann[3], T. Zhang[3] and JET EFDA contributors*

JET-EFDA, Culham Science Centre, OX14 3DB, Abingdon, UK

[1]EURATOM/CCFE Fusion Association, Culham Science Centre, Abingdon, Oxon, OX14 3DB, UK
[2]Associazione EURATOM-ENEA sulla Fusione, Consorzio RFX Padova, Italy
[3]Forschungszentrum Jülich GmbH, Association EURATOM-FZ Jülich,Germany
[4]Division of Fusion Plasma Physics, School of Electrical Engineering, Royal Institute of Technology, Association EURATOM-VR, Stockholm, Sweden
[5]Association EURATOM-Belgian State, Koninklijke Militaire School - Ecole Royale Militaire, B-1000 Brussels Belgium
[6]Max-Planck-Institut für Plasmaphysik, EURATOM-Assoziation, D-85748 Garching, Germany
** See annex of F. Romanelli et al, "Overview of JET Results", (23rd IAEA Fusion Energy Conference, Daejon, Republic of Korea (2010)).*

Preprint of Paper to be submitted for publication in
Plasma Physics and Controlled Fusion

ABSTRACT

Experiments to balance the density pump out effect during ELM control through the application of an n = 1 magnetic perturbation in Type-I Hmode plasmas at JET are presented, describing the effect on T_e, n_e and p_e profiles. Reference discharges during H-mode with and without RMP are first considered, and compared to results obtained in previous work. Pellet and gas injection are the two applied techniques; on the basis of previous experience, various particle fuelling rates have been tested on two different divertor configurations, finding those for which the compensation takes place. In terms of plasma confinement, while core pressure is found to be almost unvaried with the particle fuelling, the edge pressure pedestal improves towards the value obtained during the H-mode without the application of the magnetic perturbation. The edge stability analysis shows that the mitigated edge plasma even with the addition of particle fuelling is in the stable region against the Type-I ELM triggering peeling-ballooning modes.

1. INTRODUCTION

The active control of Edge Localized Modes (ELM) occurrence during H-mode plasmas is one of the most challenging issues in present tokamak experiments. With the ITER perspective, the power heat load caused by an ELM burst may have harmful impact on plasma components (especially on the divertor target plates) reducing their lifetime with significant erosion at every ELM. Thus, intensive ELMs must be avoided by keeping $\Delta W/W_{ped} < 1\%$ corresponding $1MJ/m^2$ tolerable deposited energy density [1]. In last years, various techniques have been approached and tested with the aim of maintaining the high confinement of plasmas in the Type- I H-mode regime and simultaneously reducing or avoiding large ELMs [2, 3, 4]. Among these, the most promising and successful consist in generating an ergodic layer in the outer edge plasma region, applying an external Resonant Magnetic Perturbations (RMP) [5]. This layer affects the edge transport barrier responsible of the enhanced performance of H-mode regimes, where the high edge pressure gradients and edge currents associated to such barrier induce peeling-ballooning modes. The perturbation cause a reduction of the pressure gradient, and this can stabilize peeling- ballooning MHD modes responsible for type I ELMs [6].

On JET, Type-I ELMs have been mitigated using a static RMP field generated by the ex-vessel Error Field Correction Coils System (EFCC) [7, 8]. The system is composed by four identical square shaped coils (approximately 6m a side), mounted between transformer limbs and each spanning a 70^o toroidal angle, at a height symmetrical with respect to the equatorial plane of the machine. The coil system can be wired in n = 1 or n = 2 configurations, modifying the relative phasing of the currents in the four coils. The n = 1 spectrum is produced when toroidally opposite coils have oppositely directed currents. With the same current level in the coils, four orientations of the resulting radial field vector with respect to the vacuum vessel (called phases) are possible, defined by the combination of two current directions in the two pairs of coils. The experimental application of both n = 1 or n = 2 RMPs gave promising results on JET. By adjusting the external perturbation amplitude both the ELM frequency and the ELM amplitude can be controlled [9]. So far, only ELM control has been obtained. A full ELM suppression is yet to be achieved in JET.

To fully comprehend the effect of the RMP on edge confinement and ELM dynamics, accurate measurements of the pedestal pressure and pressure profile are required. The set of JET diagnostics for measuring electron temperature T_e and density n_e both in the core and at the edge provides enough spatial and time resolution. In previous experiments [10], the detrimental effect of the ELM on pedestal confinement was greatly reduced during the application of the $n = 1$ ergodising perturbation, with an increased T_e edge barrier, and a density pedestal drop after the ELM reduced to less than 5%. The mitigation correlates with a reduction of the edge pressure gradient (due to both a reduced height and an increased width of the edge pressure transport barrier), consistently with the linear ELM stability theory. The large Type-I ELMs with a wide intermediate-n peeling-ballooning mode is replaced by a narrow low-n peeling mode that is driven only by the current density. Nevertheless, the pressure gradient degradation was difficult to accurately quantify, because of the limited statistics and of the experimental uncertainties. These first results on the edge pedestal region were limited, in fact, to the initial phase lasting 3s of RMP application, since the availability of space-resolved pedestal measurements (mostly from the High Resolution Thomson Scattering diagnostic) in a narrow time window of 1s.

2. EXPERIMENTAL AND ANALYSIS TOOLS

This section briefly describes the kind of experiments performed on JET to investigate the possibility of counterbalancing the above described density pump-out effect, then briefly introduces the main diagnostics used and finally describes the analysis methodology applied in the following sections.

2.1. THE EXPERIMENTS

The density pump-out is a side effect of the RMP which is found also in other tokamaks where this ELM control technique is applied [11]. The effect consists of plasma density decrease at all radii occurring during the beginning of the ergodisation phase. After that the density settles to a lower value. In these experiments the density decrease was counter balanced with additional particle fuelling, testing the effect during the mitigation phase of:

(1) The injection of different size pellets;
(2) Gas puffing of different intensity.

2.2. METHOD OF ANALYSIS

Measurements from the High Resolution Thomson Scattering (HRTS) diagnostic are used to get a more accurate T_e and n_e profile in the pedestal region to provide a full electron pressure (p_e) profile. The spatial resolution of the HRTS is 1.5cm all along the outer radius, with a time resolution of 20Hz. Measurements are mapped onto the radial midplane along flux surface provided by the EFIT code and are then fitted to provide a global analytical fit used in the analysis. Two different regions have been separately fitted, the edge ($\rho>0.8$) and the core ($\rho<0.8$) where ρ is the normalised poloidal flux, imposing continuity on fitting functions and on their derivatives at the boundary. Points in the core region are fitted with a polynomial function, because no internal transport barrier is present

in the experiments considered in this paper. As commonly done, the edge profiles are modelled with the modified hyperbolic tangent function, whose five parameters are used to quantify edge barrier properties. The effect of the EFCC external perturbation field and of the density pump-out compensation technique is studied in terms of changes of pedestal height, width and position, with the respective associated standard deviation obtained from the error matrix.

Each profile is associated with the nearest previous ELM as determined by the onset of the ELM spike in the inner divertor D_α signal. The start of an ELM is defined as the foot of the D_α onset, indicated as $\Delta t_{ELM} = 0$s, while the period is defined as the time occurring to the next ELM spike. This definition will be used throughout the rest of the paper. This method requires regular ELMs (in frequency and amplitude), a prerequisite for applying this method on the low sampling rate HRTS data that is satisfied during the H-mode discharges here considered. During the RMP phase without additional particle fuelling, only the 3s flat-top of the EFCC current are considered, avoiding the ramping phase were ELMs features evolve. During pellet injection or gas filling, the time interval is selected differently, but it will be discussed more in detail in the next sections. With this method, edge pedestal parameters time evolution can be studied with respect to the ELM phase. However, in most cases profiles from different discharges must be compared to study the effect of the mitigation and of the different density pump-out compensation techniques. The measurements in each time window are then sorted with respect to the ELM spikes, and then only measurements falling in the last 30% of the ELM period are selected. This allows comparing profiles before the occurrence of the ELM, while less affected by the features of ELMs.

2.3. STABILITY ANALYSIS

We recreate the experimental plasma equilibrium by using the measured T_e and n_e profiles (and assuming $T_i = T_e$) to calculate the self consistent bootstrap current using formula from [12]. Using the current and pressure profiles as well as the plasma shape from EFIT reconstruction, we calculate a fixed boundary equilibrium with the HELENA code [13]. This equilibrium is then used as a basis for stability analysis with the ELITE code [14]. In the stability analysis we vary the pressure gradient and the edge current density from the experimental equilibrium values to find the boundaries that limit the edge stability. The relative position of the experimental point with respect to the stability boundaries can then be used to determine if the experimental plasma is close to becoming unstable. Also the most unstable mode at the stability boundary gives indication of the character of the instability (mode number and eigenfunction) that is likely to act as a ELM trigger in the plasma.

3. REFERENCE DISCHARGES WITH AND WITHOUT RMP

On JET, previous experiments have shown that the compensation of density pump- out effect with $n = 1$ field can be achieved by means of gas fuelling [15]. An optimised gas fuelling rate to compensate the density pump-out effect without an additional drop in the plasma stored energy has been identified by means of gas fuelling up to a Greenwald fraction of 0.73 in a ITER-like shaped plasma. Depending on the configuration of target plasmas the optimized gas fuelling rate can be

different in value. Recently, the compensation of the density pump out effect due to the application of the n = 1 field has been demonstrated using both gas puffing and pellet injection [16].

Figure 1 shows the overview of the reference discharge (JET Pulse No: 77324, $I_p = 2.0$MA, $B_t = 1.85$ T). The Type-I ELMy H-mode plasma with a low triangularity shape ($u \approx 0.2$) was sustained by Neutral Beam Injection (NBI) with a total beam power of 12MW for about 10s. To increase the pump efficiency, the out strike point is located near the louver of the outer divertor.

The edge pedestal behaviour is described in Fig. 2. As the ELM occurs, both T_e and n_e pedestal height decrease, then recovering during the ELM period (first row in Fig.2). The pedestal width evolution (shown in the second row) is relatively large just after the ELM, reaching values up to 15cm. But while the density and pressure widths recover fairly quickly (time scale approximately 1-2ms), the temperature width reaches its pre-ELM value (on average) in approximately 20ms. An example of profiles is shown in the last row of Fig.2 (JET Pulse No: 77324), where measurements in a narrow time window at the beginning and at the end of the ELM cycle have been binned together.The profile drop due to the ELM (the maximum pressure gradient decreases by about 35%, from 230kPa/m to 145kPa/m) penetrates up to $\rho = 0.75$ into the plasma, with extensive release of plasma energy.

To study the effect of the ELM on the edge equilibrium, we analyze the edge stability of the plasma using the ELITE code [14] before the occurrence of the ELM he most unstable phase) and after it (the most stable phase). is that in the stability diagram (the average edge current density and the normalized edge pressure gradient), at the occurrence of the ELM the edge moves from the intermediate-n peeling-ballooning boundary deep into the stable region (see Fig.3). As the pressure gradient increases during the ELM cycle, the edge plasma reaches the intermediate-n peeling-ballooning boundary again. This behaviour is very much in agreement with most edge stability studies for type I ELMs.

As the RMP is applied (see Fig.4, JET Pulse No: 77342), during the 3s flat-top current (I_{EFCC}), the ELM effect on the plasma edge is reduced. ELM control started in the I_{EFCC} ramp up phase once the EFCC current exceeded a threshold value (about 16kAt, the IEFCC amplitude was kept below the threshold value for the excitation of a locked mode), with the ELM frequency increasing from 15Hz to 30Hz. The mitigation was sustained during the following flat-top, which is almost a factor 10 longer than the plasma energy confinement time and which is limited only by the EFCC power supply. After the ramp-down phase, ELMs were not mitigated anymore and they appeared again with their lower frequency. The pedestal evolution variation between the phase without and with RMP is shown in Fig.5. Since the ELM frequency is doubled, the pedestal cycle lasts 30 ms instead of 60ms. The density pump-out decreases the density pedestal height, while the temperature pedestal height reaches a higher value as expected, since the entire T_e profile increases at the RMP application. The effect of an ELM on the density pedestal heights is reduced, with a density drop from 30% to 15% at the ELM spike. The temperature drop is still reduced after the ELM, but with a more significant spread of HRTS points which does not allow quantifying it. However, the Electron Cyclotron Emission (ECE) heterodyne radiometer system gives a reasonably good measure for the pedestal temperature drop during an ELM. At the top of the pedestal the drop is reduced from 30% to 15% when the EFCC is applied. Within the standard deviation, no significant difference

is found in the pedestal width (see second row in Fig.5). The density width recovers immediately, while temperature width still needs a considerable fraction of the ELM cycle. The effect of the perturbation on the pressure profile can be appreciated comparing the edge profile in the last 30% of the ELM cycle in the phase without and with RMP (Fig.6). The maximum pressure gradient decreases by about 40%, from 230kPa/m to 140kPa/m.

A quantitative comparison of all pedestal parameters can be found in Table 1. The values correspond to the averaged parameters for the profiles in the last 30% of the ELM cycle. The errors are the profile to profile standard deviations. For the temperature profiles, the pedestal heights are approximately similar, while the width seems slightly larger when I_{EFCC} is applied. However, due to the spread of the data (see Fig. 5b) conclusive claims are not possible. Concerning density and pressure, the height at the pedestal are lower when the I_{EFCC} is applied while the width is similar. This implies that the gradient reduction during the I_{EFCC} phase can be mainly ascribed to the decrease in density and pressure at the pedestal. As a general consideration, the temperature is always affected by a larger uncertainty. This is due to the temperature profile shape with respect to the density one, as a less defined pedestal height and a narrower width make single profile fits more critical, also with binned profiles. To limit this uncertainty, in this pulse a small plasma sweeps of 1.5cm was applied during the RMP phase in order to increase the spatial resolution of HRTS measurements [17]. Once profiles are binned, this increases the sampling of the very steep pedestal region.

The energy loss during an ELM ΔW_{ELM}/WELM is calculated using the temperature and the density profiles by considering both the conductive and the convective losses. When the IEFCC is applied the energy losses are 50% lower.

For these measurements the stability analysis shows that the application of RMP positively affects the edge stability (see Fig.7), moving the experimental point in the stability diagram (magenta star) from the vicinity of the stability boundary deep into the stable region (yellow star). These results lack of consistency with our experimental observations, since the common picture of type-I ELMs [18] is that during an ELM a transition in the stability diagram from a stable to an unstable region occurs, with the edge destabilized by either peeling or ballooning modes, or both. In our previous work [10], the mitigation was correlated with a reduction of the edge pressure gradient, and the Type-I ELMs correlated with a wide intermediate-n peeling-ballooning mode replaced by a narrow low-n peeling mode. The location of the stability point at the peeling boundary with instabilities driven by the current density explained that ELMs were still present and not completely suppressed. In the present case, the transition to a completely stable region should mean a complete ELM suppression, which is not the case. In fact, the change in the edge stability is similar to what is observed in DIII-D during the full suppression of ELMs [19].

An explanation could be found in three dimensional equilibrium effects not included in the ELITE code which consider only axisymmetric ideal MHD instabilities. The RMP application causes a 3D deformation of the plasma column, as already shown in [10] and reference therein, with the appearance of toroidally localized pressure gradient increase that might destabilize ELMs and that would change the stability diagram. This possible solution to the inconsistency between experiments and models will be investigated in future works.

As seen in Fig.1 at the end of the EFCC application, there is a short ELM free period before the Type I ELMs return. We do the stability analysis using single time point profiles in the beginning and at the end of the ELM free period. As can be seen in Fig. 8 when the EFCC is turned off the edge plasma remains deep in the stable region but then returns close to the intermediate-n peeling-ballooning boundary just before the Type I ELMs start again. This indicates that during the EFCC operation the edge plasma is indeed stable against axisymmetric instabilities and would be ELM free if some other, possibly three dimensional instability were not triggered. It must be noted that the error margins for the profile parameters in a single time point analysis are larger than shown in Table 1 due to smaller number of data points in the fit.

4. DENSITY PUMP-OUT COMPENSATION WITH PELLET INJECTION

The effect of particle fuelling with pellet injection during RMP application is studied using three different pellet lengths, to consider different re-fuelling rate, each with its own injection frequency determined by the injector performance: 4mm and 3.5mm at 10 Hz and 3mm at 8Hz. Pellets started being injected at the beginning of I_{EFCC} flat-top, after the 0.5s of I_{EFCC} current ramping phase. The criterion for comparing profiles with the plasma in a more stable condition is satisfied in the case of pellet injection if HRTS measurements fell: (a) in the last 30% of the ELM cycle, (b) after the ablation of the pellet and (c) once the average density (i.e. the line integrated density) does not vary from pellet to pellet. This latter constraint means that the effect of the pump out is balanced by the particle fuelling. Constraints (b) and (c) narrow the considered time window for the RMP and pellet phase, reducing the number of available measurements to a few.

In figures 9 and 10, the results for the 4mm and 3.5mm pellet sizes are shown. In the bottom frames a and c, the $D\alpha$ and line integrated core density are used to qualitatively follow the RMP onset during the H-mode (I_{EFCC} in frame b) and the subsequent pellet injection phase. On the top frames, the global and pedestal T_e, n_e and peprofiles are shown for the time points during the H-mode without RMP (red), with RMP (green) and with RMP and pellet (blue). The dynamic plasma behaviour with 4mm and 3.5mm pellets is similar. As the RMP is applied, ELM frequency is doubled with reduction of amplitude. The density pump out causes a strong density decrease and a simultaneous temperature increase, both in the core and at the edge, with a global reduction of plasma pressure (and hence confinement). Then, pellet injection completely recovers the density and at the same time cools down the plasma temperature below the value prior to RMP. The pressure profile is only partially improved, since the core pressure is unvaried with pellet injection, while the edge the pressure pedestal height is between the prior and during RMP value. On the contrary, the 3mm size pellet does not compensate the pump out effect (data not shown in the paper). Both the profile and the line integrated density stabilize to a value intermediate between that before the RMP application and before the pellet injection. Furthermore, the 3 mm pellet fuelling does not recover the edge pressure.

The pump-out recovery with pellet injection was tested also with a different magnetic configuration, with magnetic field lines on the divertor slightly displaced towards a region were fast IR camera can be use to estimate heat flux measurement (strike point on tile 5). With this configuration, the effect of

RMP on ELM control and edge pedestal behaviour is similar to the case shown in Section 3, while the effectiveness of pellet injection on the density recovery is different. A 3.5mm pellet increases the density to a value which exceeds that before the RMP application, while a 3mm pellet recovers the density to the level before RMP application. This is shown in Fig.11, where the density change from pellet can also be compared to the intensity of the pump-out effect (consider the cases without and with the application of the RMP). A change in divertor configuration has led to a change in particle recycling, requiring a change in the particle source from pellets in order to balance the particle loss due to the pump-out. We can conclude that the required particle fuelling rate using pellets to compensate the density pump-out effect depends on the divertor configuration.

5. DENSITY PUMP-OUT COMPENSATION WITH GAS FILLING

Gas fuelling was tested with two fuelling rates, 8×10^{21} and 12×10^{21} electrons per second (el/s), repeating the discharge JET Pulse No: 77327 (with the outer strike point located near the louver of the outer divertor and with RMP applied). The analysis accomplished is similar to that presented in the previous section. The main difference is that particles are not injected in a short pulse, as in the pellet case, but continuously. This means that the plasma is never in a perturbed state. Thus, the constraints on profiles selection deals only with (a) the ELM phase and (b) the reaching of the balance between the pump out and the particle fuelling, being monitored through interferometer measurements. The condition (b) is reached in less than a second with pellet injection, while gas fuelling takes about twice the time, due to a deeper particle penetration with pellet injection, and profile analysis can be accomplished only in the last phase of the EFCC current flat-top. Therefore, also in this case the number of available profiles is limited. In Fig.12, the time evolution of the line integrated density is shown for pulses with pellet and gas fuelling.

The lower fuelling rate (8×10^{21}el/s) does not recover the density completely, while the higher (12×10^{21}el/s) achieves full compensation of the pump-out. For the higher rate (profiles shown in Fig.13), the effect on the electron profiles is similar to the pellet case. The density recovers and temperature decreases all along the entire profile, a reduced but still present enhancement in edge pressure pedestal height to a value in between that had before and during application of the RMP. The global confinement is reduced by 20-30%.

CONCLUSIONS

We have described the effect on T_e, n_e and p_e profiles of two different techniques for the compensation of the density pump out effect occurring during Type-I ELM control experiments with resonant magnetic perturbation fields on JET. We first characterized profiles measured during a standard H-mode discharge, in terms of the edge pedestal height evolution during an ELM cycle obtained from the reordering of profiles with respect to the nearest previous ELM. The effect of the RMP application is then quantified, applying a similar method, and comparing profiles in the last 30% of the ELM cycle. The results obtained in a previous work are confirmed. The edge pressure height decreases with a consequent decrease of the edge pressure gradient. This is also consistent with the observation of the pressure pedestal height recovery during the ELM cycle with the RMP application.

The pressure pedestal height with RMP follows the same evolution as that without RMP in a shorter cycle, since the ELM with RMP has a higher frequency. One could interpret this behaviour as a reduction of the threshold at which the instability responsible for the occurrence of the ELM is destabilized by the edge pressure gradient due to the changes in edge plasma configuration. However, the stability analysis shows that compared with the reference ELMy H-mode plasma, during the mitigation the static magnetic perturbation moves the operational point to a more stable region before the occurrence of an ELM. Furthermore, while both pellets and gas injection increase the edge pressure gradient, the edge stays still deep in the stable region against the peeling-ballooning modes with stability diagrams similar to Fig. 7. This is partially inconsistent with the experiment, since being far from peeling and ballooning instabilities do not explain the occurrence of the ELM instability, assuming that pressure and current are the only causes triggering it. On the basis of stability diagrams, additional mechanisms might be considered and investigated to explain why no full ELM suppression was achieved, such as those ascribable to 3D effects.

Pellet injection and gas fuelling have been found reliable techniques to balance the pump-out effect during the RMP application and recovering the density profile measured before the onset of the perturbation. The temperature profile is cooled by the particle fuelling. However, the resulting pressure profile does not change in the core but only at the edge, where the pedestal height gets an intermediate value between those before and during the RMP. For both fuelling methods a minimum fuelling rate (i.e., proper pellet size or gas injection rate) is found for the effective density compensation. The required fuelling rate depends on the divertor configuration, i.e. on the change in particle recycling and fuelling efficiency. Also for both fuelling methods, the resulting edge temperature when the density pump-out is fully compensated remains below the value before the RMP.

ACKNOWLEDGMENTS

This work was supported by EURATOM and carried out within the framework of the European Fusion Development Agreement. The views and opinions expressed herein do not necessarily reflect those of the European Commission.

REFERENCES

[1]. Loarte A. et al., Nuclear. Fusion **47**, S203–S263 (2007).
[2]. Lang P.T. et al. , Nuclear. Fusion **43**, 1110 (2003).
[3]. Degeling A.W. et al., Plasma Phys. Control. Fusion **45**, 1637 (2003).
[4]. Maddison G.P. et al., Plasma Phys. Control. Fusion **45**, 1657 (2003).
[5]. Evans T. et al., Nature Phys. **2**, 419 (2006).
[6]. Tokar M.Z. et al., Physics. Rev. Lett. **98**, 095001 (2007).
[7]. Barlow I. et al., Fusion Engineering and Design **58-59**, 189 (2001).
[8]. Liang Y. et al., Physics. Rev. Lett. **98**, 265004 (2007).
[9]. Liang Y. et al., Plasma Physics. Control. Fusion **49**, 581 (2007).
[10]. Alfier A. et al., Nuclear. Fusion **48**, 115006 (2008).
[11]. Evans T.. et al., Nuclear. Fusion **48** 024002 (2008).

[12]. Sauter O., Angioni C and Lin-Liu Y R, Phys. Plasmas **6**, 2834 (1999).
[13]. Huysmans G.T.A., Goedbloed J.P., Kerner W.O.K., Computational Physics (Proc. Int. Conf. Amsterdam, 1991),World Scientific Publishing, Singapore, **371** (1991)
[14]. Wilson H.R., Snyder P.B., Huysmans G.T.A. and Miller R.L., Physics. Plasmas **9**, 1277 (2002).
[15]. Liang Y. et al., Journal of Nuclear Materials **390–391**, 733–739 (2009).
[16]. Liang Y. et al., 36th EPS Conference on Plasma Phys. Sofia, June 29 - July 3, 2009 ECA Vol.33E, O-5.062 (2009).
[17]. Beurskens M et al, Nuclear. Fusion **49**, 125006 (2009).
[18]. Snyder P.B. et al.,Physics. Plasmas **9**, 2037 (2002).
[19]. Burrell K.H. et al. Plasma Physics. Control. Fusion **47**, B37 (2005).

	w/o I_{EFCC}	*with* I_{EFCC}
T_e *(keV)*	*1.0 ± 0.1*	*1.0 ± 0.2*
w_{Te} *(cm)*	*1.8 ± 0.7*	*3.2 ± 0.9*
∇T_e *(keV/m)*	*60 ± 20*	*30 ± 15*
n_e $(10^{19}m^{-3})$	*3.2 ± 0.2*	*2.1 ± 0.2*
w_{ne} *(cm)*	*2.9 ± 0.4*	*2.8 ± 0.3*
∇n_e $(10^{19}m^{-3})$	*110 ± 20*	*75 ± 15*
p_e *(kPa)*	*5.0 ± 0.7*	*3.2 ± 0.7*
w_{pe} *(cm)*	*2.5 ± 0.3*	*2.6 ± 0.7*
∇pe *(kPa/m)*	*200 ± 50*	*120 ± 60*
$\Delta W_{ELM}/W_{ELM}$ *(%)*	*15 ± 10*	*7 ± 5*

Table 1: Height at the pedestal, pedestal width and pedestal gradient from temperature, density and pressure, with and without I_{EFCC}*. The gradient is calculated as the ratio between height and width (its error is therefore larger than those shown in Fig. 6, being representative of all the pedestal width). The last row shows the energy lost during ELMs.*

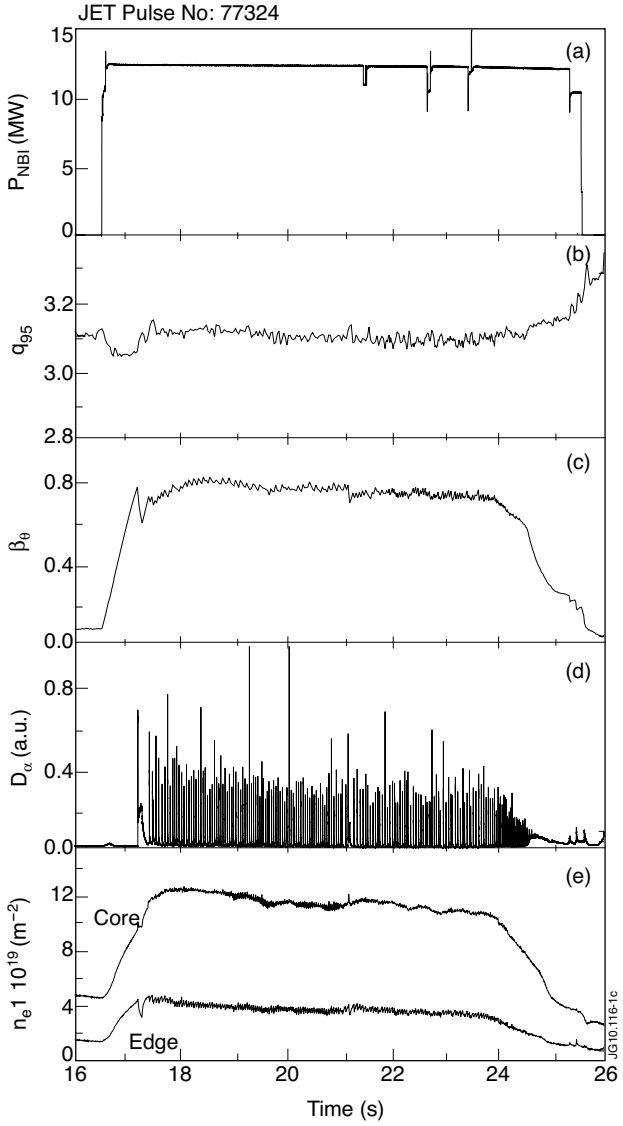

Figure 1: Time evolution of reference plasma discharge JET Pulse No: 77324.

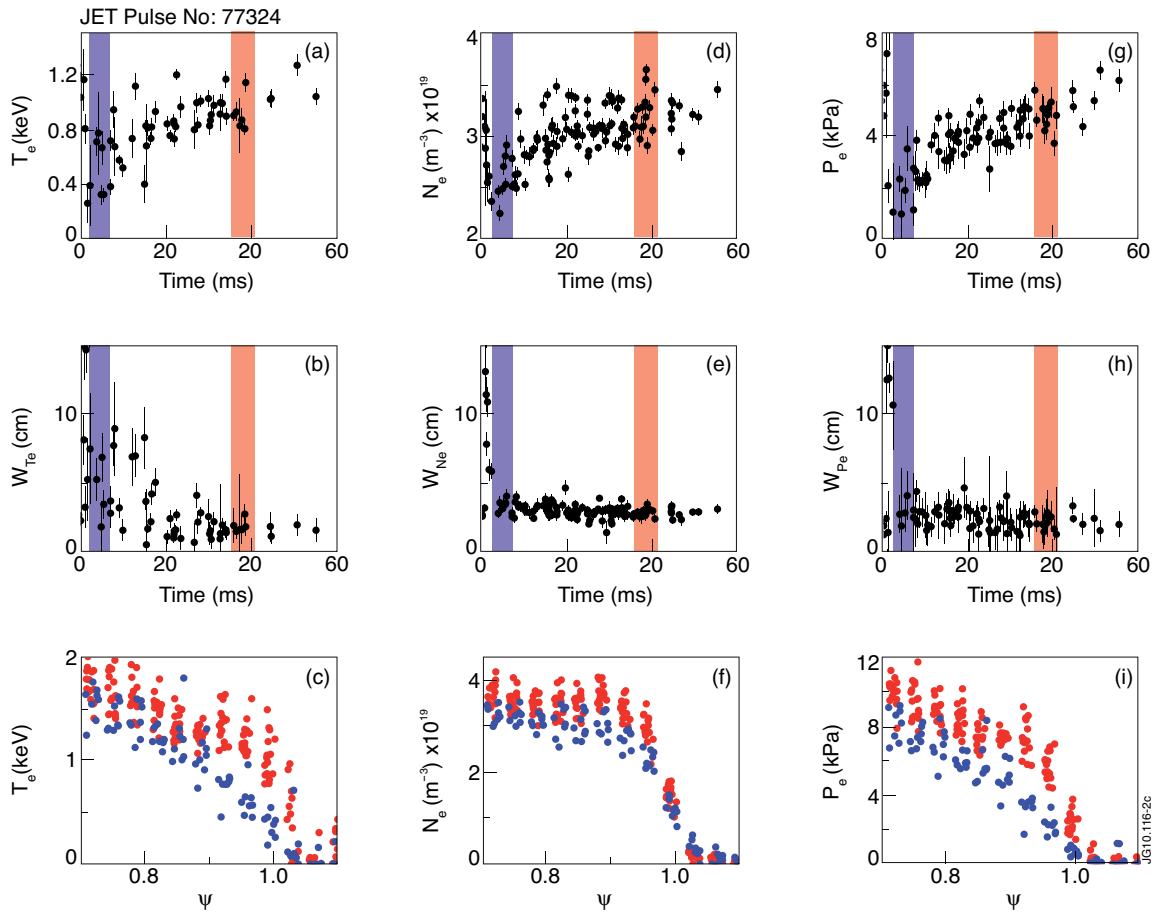

Figure 2: (Top) Pedestal height and (middle) width evolution in an ELM cycle for T_e, n_e and p_e JET Pulse No: 77324. (bottom) profiles in (blue) the initial and (red) final phase of the ELM cycle show the effect of an ELM on the edge.

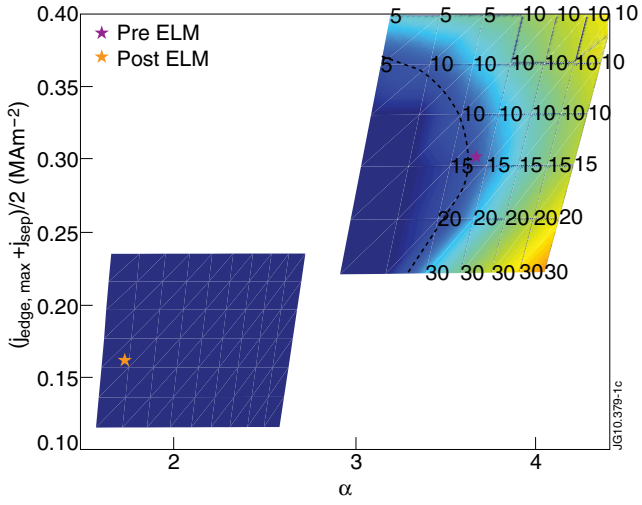

Figure 3: The edge stability diagram of the Type I ELMy reference discharge using profiles taken just before and right after an ELM. The x-axis is the normalised pressure gradient and the y-axis is the average current density in the edge region. The color represents the growth rate of the mode. The blue region is stable.line) and 69093 (dashed dotted line).

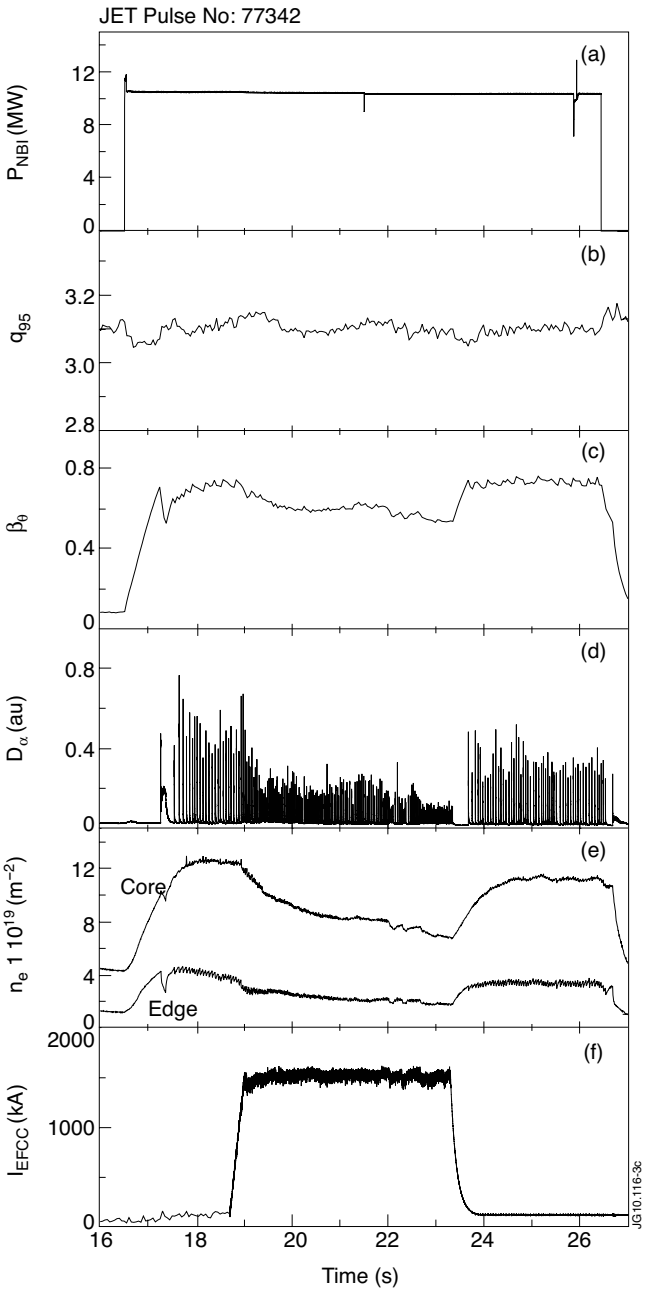

Figure 4: Time evolution of reference plasma discharge JET Pulse No: 77342.

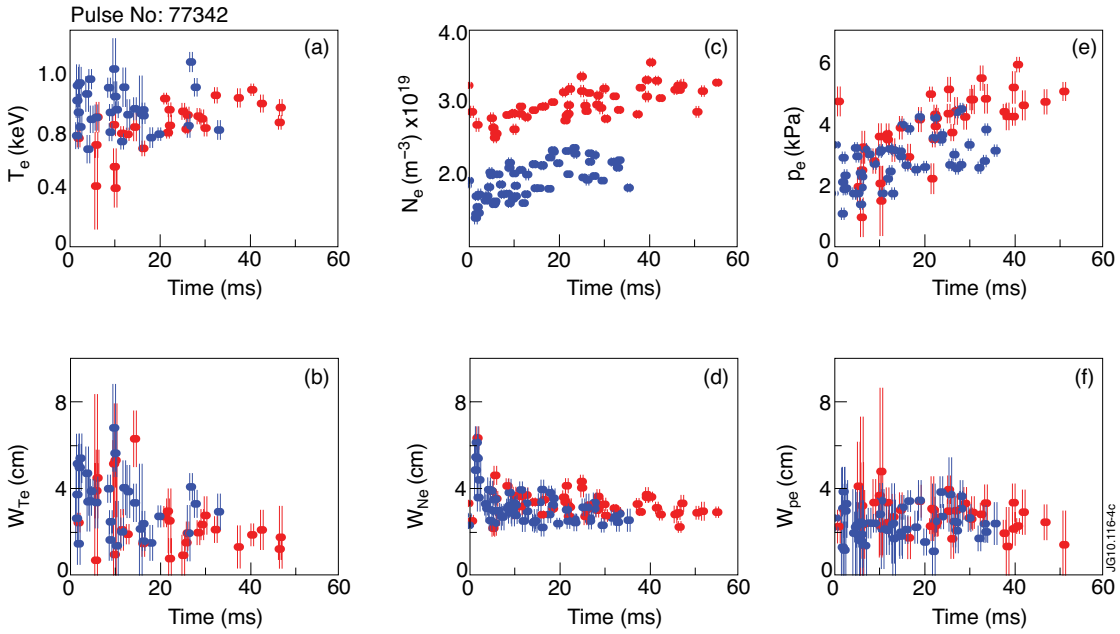

Figure 5: JET Pulse No: 77342. (top) Pedestal height and width evolution in an ELM cycle for T_e, n_e and p_e without and with RMP (red and blue circles).

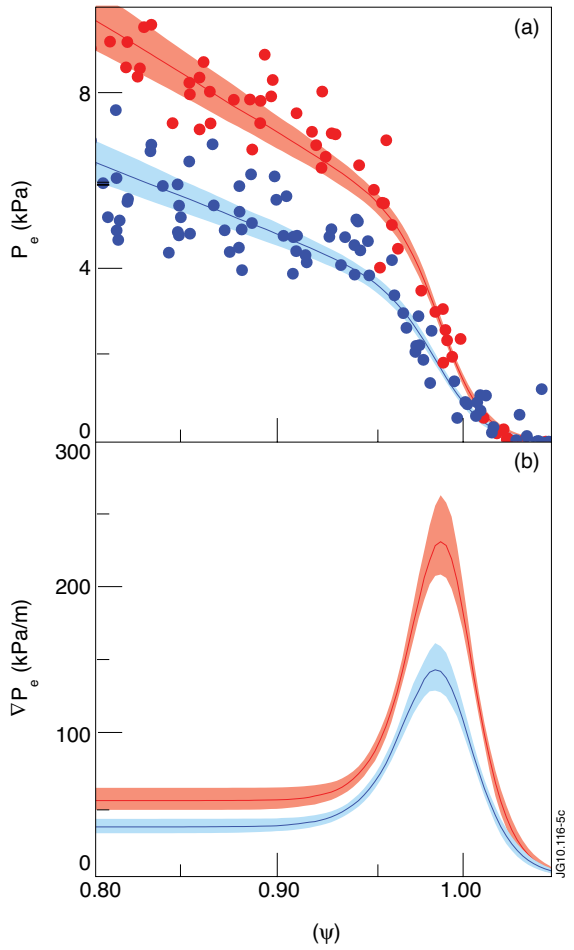

Figure 6: Edge pressure profiles (top) in the last 30% of an ELM cycle, and correspondent pressure gradient (bottom), without and with RMP (blue and red circles). Data are obtained in JET Pulse No: 77342 with the 1.5 cm plasma ROG sweep: a higher sampling of the edge pedestal region can be appreciated.

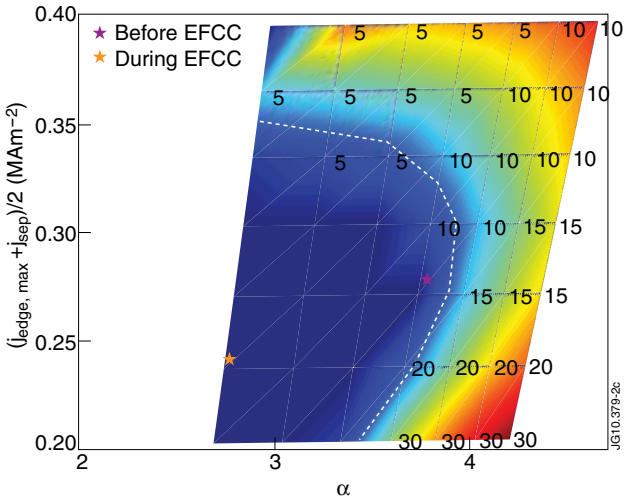

Figure 7: Edge stability diagrams of of JET Pulse No: 77342 discharge before and during the EFCC mitigation phase for profiles shown in Fig. 6.

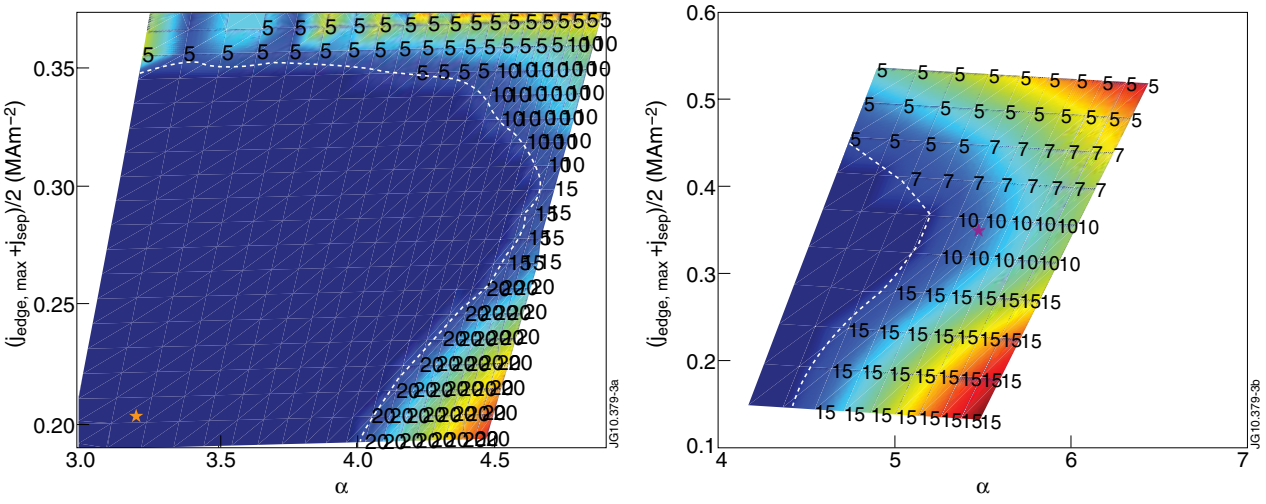

Figure 8: Edge stability diagrams of JET Pulse No: 77342 discharge at (a) 23.403s (beginning of the ELM free period) and (b) 23.603s (end of the ELM free period).

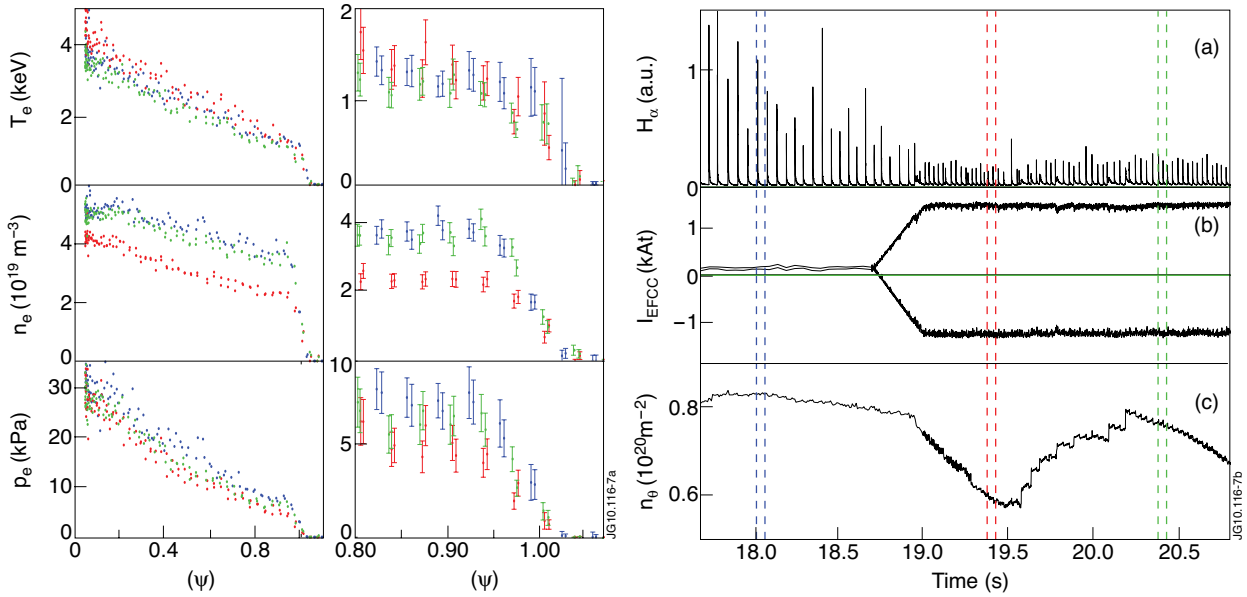

Figure 9: (Top) T_e, n_e and p_e full and edge profiles with 4mm pellet injection at 10Hz: before RMP (blue), with RMP (red) and with RMP and pellet (green), JET Pulse No: 77327. (Bottom) Dα, EFCC current, core line averaged density; time instant of HRTS profiles are shown.

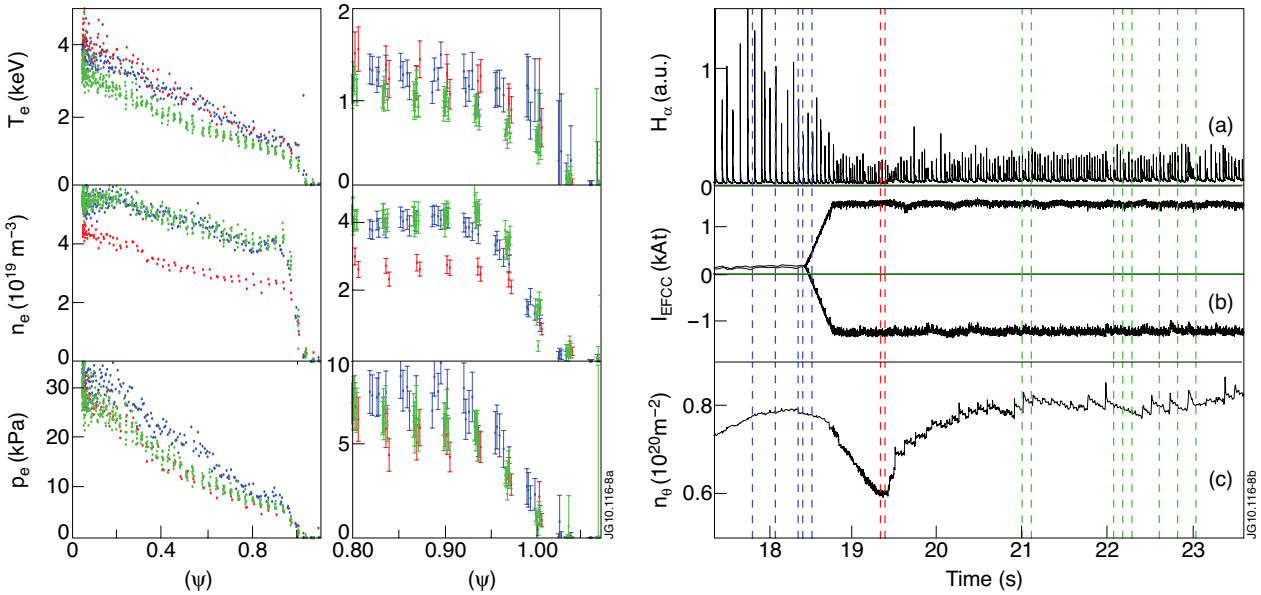

Figure 10: (Top) T_e, n_e and p_e full and edge profiles with 3.5mm pellet injection at 10Hz: before RMP (blue), with RMP (red) and with RMP and pellet (green), JET Pulse No: 77331. (Bottom) Dα, EFCC current, core line averaged density; time instant of HRTS profiles are shown.

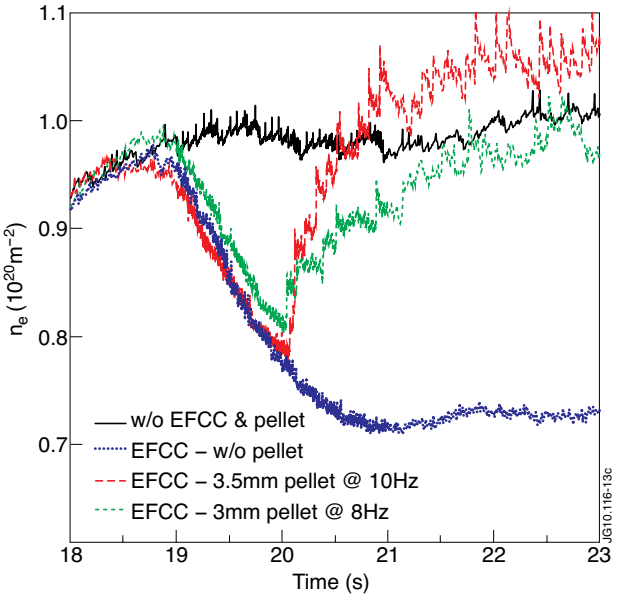

Figure 11: Line integrated density measurements with and without RMP, and with 3.5mm and 3mm pellets with RMP. Strike point is on tile 5.

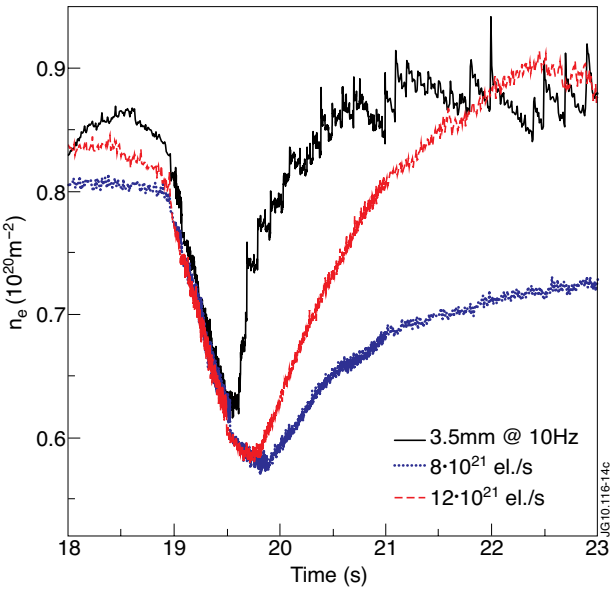

Figure 12: Comparison between line integrated density measurements with 3.5mm pellet injection, 8 × 10^{21}el/s and 12 × 10^{21}el/s gas fuelling rate.

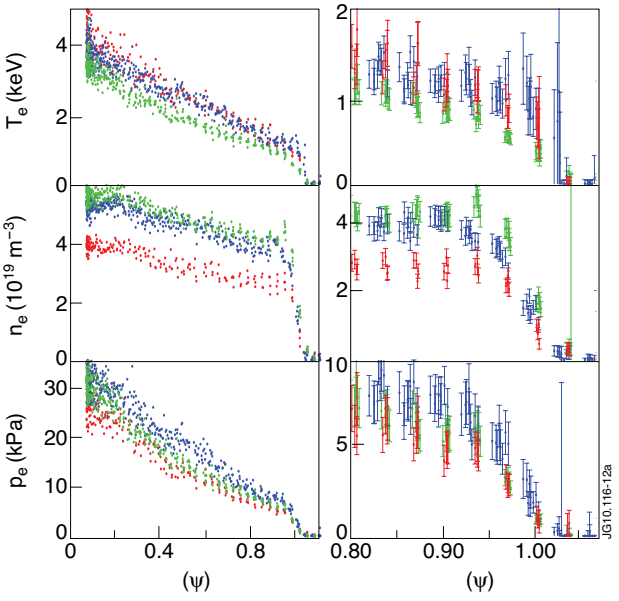

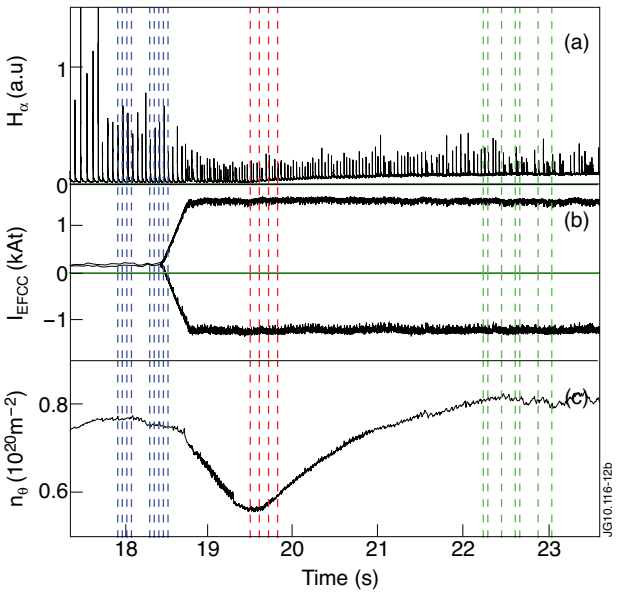

Figure 13: J(Top) T_e, n_e and p_e full and edge profiles with 12 × 10^{21} el/s gas fuelling rate: before RMP (blue), with RMP (red) and with RMP and gas fuelling (green), JET Pulse No: 77335. (bottom) Dα, EFCC current, core line averaged density; time instant of HRTS profiles are shown.